A Novel Block Method for Analyzing a Fractional Dynamics of CD4+T Cell in HIV-Infected Individuals

Nursyazwani Mohamad Noor, Siti Ainor Mohd Yatim and Iskandar Shah Mohd Zawawi

***Abstract*—This paper describes the development of a novel fourth-order 2-point fractional block method with a variable step size to approximate the solutions of fractional model of HIV infection in CD4$^+$T cells. The method is developed using a fractional linear multistep formula as the basis function. The necessary conditions for the convergence test and stability analysis of the method are presented. The study indicates that the method converges, and its stability region exhibits A-stability for various fractional order, α. Numerical experiments are presented to demonstrate the efficiency and accuracy of the new method in comparison to existing methods in the literature. The simulation results reveal that memory effects significantly influence the progression of HIV infection by delaying the peak viral load and altering the stability behavior of the system, which cannot be captured by classical models. The proposed method offers an alternative solver for fractional-order dynamical systems with memory effects, with potential applications in modeling other biological phenomena such as disease transmission.**

***Index Terms*—Linear multistep method, fractional block method, fractional order, stability, CD4$^+$T-cell, HIV infection.**

I. Introduction

HUMAN immunodeficiency virus (HIV) is a retrovirus that generates acquired immunodeficiency syndrome (AIDS) in humans, as indicated by medical definitions, clinical findings, and virology analysis [1]. According to [2], the global HIV epidemic remains a substantial public health challenge, with an estimated 39.9 million individuals living with HIV in 2023. The HIV epidemic continues to persist, disproportionately affecting specific populations, despite the progress made in prevention and treatment. HIV disproportionately affects women and girls, who represent 53% of the HIV-positive population. 1.4 million children aged 0-14 years currently live with HIV, which remains a concern. The need for better counseling and testing services is underscored by the fact that a substantial number of people living with HIV do not know their status. In numerous regions, access to antiretroviral therapy (ART) remains a challenge, particularly for marginalized and vulnerable populations. The HIV epidemic causes far-reaching repercussions, including increased mortality, economic hardship, and social stigma. A multifaceted approach that addresses both biological and social determinants of health is necessary to address the HIV epidemic.

Manuscript received January 31, 2025; revised May 16, 2025.

This work was supported by the Ministry of Higher Education Malaysia through the Fundamental Research Grant Scheme 2024 (FRGS/1/2024/STG06/UITM/02/3).

N. M. Noor is a lecturer of School of Quantitative Sciences, College of Arts and Sciences, Universiti Utara Malaysia, 06010 UUM Sintok, Kedah, Malaysia. (e-mail: nursyazwanimn@uum.edu.my).

S. A. M. Yatim is a senior lecturer of School of Distance Education, Universiti Sains Malaysia, 11800 USM Gelugor, Pulau Pinang, Malaysia. (Corresponding author, e-mail: ainor@usm.my).

I. S. M. Zawawi is a senior lecturer of Faculty of Computer and Mathematical Sciences, Universiti Teknologi MARA, 40450 Shah Alam, Selangor, Malaysia. (Corresponding author, e-mail: iskandarshah@uitm.edu.my).

TABLE I
VARIABLES AND PARAMETER [7].

Symbol	Description	Constant
ϖ	Source term for uninfected CD4$^+$T cells	1.0E-01/day mm^3
ψ	Natural death rate of CD4$^+$T cells	2.0E-02/day
υ	Growth rate of CD4$^+$T cells population	3.0/day
T_{max}	Maximal population level of CD4$^+$T cells	1500/day mm^3
φ	Rate of CD4$^+$T cells become infected with virus	2.7E-03/mm^3
ϱ	Blanket death rate of $I(t)$	3.0E-01/day
N	Total viral particles produced by infected CD4$^+$T cells	10/mm^3
τ	Virus's clearance rate	2.4/day

Mathematical dynamic models, which encompass the fundamental principles of analysis of manipulation and avoidance of the transmission of a variety of diseases, have been the subject of numerous attempts to design, analyse, simulate, and solve them in recent decades. In this context, the development of analytical models to investigate the dynamics of HIV infection is also recognized as a useful and effective approach [3]–[6]. These models are instrumental in capturing the interactions between viral load and immune response. Therefore, this research will consider the following system of ordinary differential equations (ODEs) to model the dynamics of the interaction between HIV and CD4$^+$T cells [7].

$$\begin{aligned} T'(t) =& \varpi - \psi T + \upsilon T\left(1 - \frac{T+1}{T_{max}}\right) - \varphi V T, \\ I'(t) =& \varphi V T - \varrho I, \\ V'(t) =& N\varrho I - \tau V. \end{aligned} \tag{1}$$

where $T(t)$ is the concentration of healthy CD4$^+$T cells at time t, $I(t)$ is the concentration of infected CD4$^+$T cells at time t, and $V(t)$ is the concentration of a virus population of CD4$^+$T cells by HIV in the blood at time t. Meanwhile, the parameters and their value for (1) are presented in Table I.

It is crucial to recognize that biological systems possess the ability to retain information and exhibit subsequent

effects. In models described by ODEs of integer order, such effects are ignored. Due to the correlation between fractional calculus and memory systems, fractional models are better suited for modeling dynamical systems [8]. Therefore, the following model is established by substituting the Caputo fractional derivative into equation (1).

$$\begin{aligned} {}^{C}D^{\alpha_1}T(t) =& \varpi - \psi T + \upsilon T\left(1 - \frac{T+1}{T_{max}}\right) - \varphi VT, \\ {}^{C}D^{\alpha_2}I(t) =& \varphi VT - \varrho I, \\ {}^{C}D^{\alpha_3}V(t) =& N\varrho I - \tau V. \end{aligned} \tag{2}$$

where ${}^{C}D^{\alpha}$ is denoted as the Caputo fractional derivative, and $\alpha \in (0, 1]$. The system (2) simulated with preliminary states $[T_0, I_0, V_0]^T = [0.1, 0.0, 0.1]^T$ for $t \in [0, 1]$. Assume that the functions of the mathematical model satisfy the necessary conditions for the existence and uniqueness of the solution of (2), as described in [9].

Several numerical methods have been developed to solve the fractional model (2), including fourth-kind Chebyshev wavelets [8], the multistep differential transform method [10], the piecewise polynomial collocation method [11], and the Newton polynomial method [12]. However, they still encounter challenges in ensuring stability and achieving computational efficiency, particularly in biological applications such as HIV infection. To address these challenges, this study develops a block method known as the block backward differentiation formula (BBDF) to solve the dynamical system (2). The BBDF method is particularly effective for equations involving non-integer solutions. These types of equations are often seen in fields such as physics and biology, where systems exhibit memory effects or long-lasting influences. It has been widely used for ODEs, especially those with stiff properties that are challenging for traditional methods to address [13]–[15]. Due to its stability and accuracy, the BBDF method can handle complex, time-dependent equations with minimal error, closely approximating exact solutions compared to other methods. Its adaptability also allows scientists to model systems with unusual patterns and behaviors. Although it can be computationally intensive due to its reliance on historical data, various adjustments enhance its efficiency and reliability.

The fractional BDF (FBDF) method has been developed by a few researchers [16], [17], but it is not a block-based approach to the solution of FDEs. The method was developed using convolution quadrature techniques, which proved to be an obstacle when attempting to incorporate the technique into a block method. Therefore, this study introduces the fractional BBDF method (FBBDF) by adopting the strategies from [14] and [18] to compute the solution for fractional HIV infection model of a CD4$^+$ T cell (2). Besides, the results of this study are intended to provide an alternative solver for other dynamical systems with memory and give the opportunities for future research on its application, such as the Covid-19 pandemic model [19], cervical cancer model [20], zika virus fever [21], etc.

The structure of this paper is as follows: The method being proposed is developed in Section II. Section III outlined the analysis of the methods by evaluating the order and error constant, assessing the convergence of the method, and examining the stability of the methods. The numerical and graphical results will be discussed in Section IV. Finally, a conclusion will be drawn in Section V.

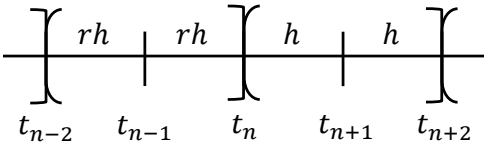

Fig. 1. Illustration for the VS2FBBDF(4) method.

II. Construction of the Method

In this section, the fourth-order fractional 2-point BBDF is constructed with variable step size. The method is referred to as VS2FBBDF(4), and Figure 1 illustrates the visual representation of the method. In the diagram, the interval rh denotes the step size of the prior block, whereas h represents the step size of the block that will be used to approximate the solution points [22].

The equation for VS2FBBDF(4) is derived by applying a variable step size approach to the 2FBBDF(4) method [23], and is defined by the linear difference operator as follows:

$$\begin{aligned} L_i\left[y(t); h; \alpha\right] =& \sum_{j=0}^{4} \gamma_{j,i} y_{n+j-2} - h^{\alpha}\beta_i f_{n+i}, \\ =& \sum_{j=0}^{4} \gamma_{j,i} y_{n+j-2} - h^{\alpha}\beta_i {}^{C}D^{\alpha} y_{n+i}, \\ =& 0, \end{aligned} \tag{3}$$

where the Taylor's series expansion of y_{n-2}, y_n, y_{n+1}, y_{n+2}, and ${}^{C}D^{\alpha}y_{n+i}$ about t_n given as follows:

$$\begin{aligned} y_{n-2} =& y_n + (-2rh)y'_n + \frac{(-2rh)^2}{2!}y''_n + \cdots, \\ y_{n-1} =& y_n + (-rh)y'_n + \frac{(-rh)^2}{2!}y''_n + \cdots, \\ y_n =& y_n, \\ y_{n+1} =& y_n + (h)y'_n + \frac{(h)^2}{2!}y''_n + \cdots, \\ y_{n+2} =& y_n + (2h)y'_n + \frac{(2h)^2}{2!}y''_n + \cdots, \\ {}^{C}D^{\alpha}y_{n+i} =& \frac{(ih)^{1-\alpha}}{\Gamma(2-\alpha)}y'_n + \frac{(ih)^{2-\alpha}}{\Gamma(3-\alpha)}y''_n + \cdots. \end{aligned} \tag{4}$$

Then, equation (4) is substituted into equation (3) yields

$$\begin{aligned} &\gamma_{0,i}\left[y_n + (-2rh)y'_n + \frac{(-2rh)^2}{2!}y''_n + \cdots\right] + \gamma_{1,i}\left[y_n\right. \\ &\left. + (-rh)y'_n + \frac{(-rh)^2}{2!}y''_n + \frac{(-rh)^2}{2!}y'''_n + \cdots\right] + \gamma_{2,i}\left[y_n\right] \\ &+ \gamma_{3,i}\left[y_n + (h)y'_n + \frac{(h)^2}{2!}y''_n + \frac{(h)^2}{2!}y'''_n + \cdots\right] + \gamma_{4,i}\left[y_n\right. \\ &\left. + (2h)y'_n + \frac{(2h)^2}{2!}y''_n + \frac{(2h)^2}{2!}y'''_n + \cdots\right] + h^{\alpha}\beta_i\left[\frac{(ih)^{1-\alpha}}{\Gamma(2-\alpha)}y'_n\right. \\ &\left. + \frac{(ih)^{2-\alpha}}{\Gamma(3-\alpha)}y''_n + \frac{(ih)^{3-\alpha}}{\Gamma(4-\alpha)}y'''_n + \cdots\right] = 0. \end{aligned} \tag{5}$$

Then we collect all the coefficients y_n, y'_n, y''_n, y'''_n, $\cdots$ in equation (5) and the following expressions are obtained as in equation (6) where

$$\begin{aligned}
C_{0,i} :=& \gamma_{0,i} + \gamma_{1,i} + \gamma_{2,i} + \gamma_{3,i} + \gamma_{4,i} = 0,\\
C_{1,i} :=& (-2r)\gamma_{0,i} + (-r)\gamma_{1,i} + \gamma_{3,i} + 2\gamma_{4,i}\\
&- \frac{(i)^{1-\alpha}}{\Gamma(2-\alpha)} = 0,\\
C_{2,i} :=& \frac{(-2r)^2}{2!}\gamma_{0,i} + \frac{(-r)^2}{2!}\gamma_{1,i} + \frac{(1)^2}{2!}\gamma_{3,i}\\
&+ \frac{(2)^2}{2!}\gamma_{4,i} - \frac{(i)^{2-\alpha}}{\Gamma(3-\alpha)} = 0,\\
C_{3,i} :=& \frac{(-2r)^3}{3!}\gamma_{0,i} + \frac{(-r)^3}{3!}\gamma_{1,i} + \frac{(1)^3}{3!}\gamma_{3,i}\\
&+ \frac{(2)^3}{3!}\gamma_{4,i} - \frac{(i)^{3-\alpha}}{\Gamma(4-\alpha)} = 0,\\
C_{4,i} :=& \frac{(-2r)^4}{4!}\gamma_{0,i} + \frac{(-r)^4}{4!}\gamma_{1,i} + \frac{(1)^4}{4!}\gamma_{3,i}\\
&+ \frac{(2)^4}{4!}\gamma_{4,i} - \frac{(i)^{4-\alpha}}{\Gamma(5-\alpha)} = 0.
\end{aligned} \tag{6}$$

To calculate the first point of the method, y_{n+1}, we substitute $i = 1$ and $\gamma_{3,1} = 1$ into equation (6). By solving the system of equation (6) simultaneously, we obtain the following coefficients.

$$\begin{aligned}
\gamma_{0,1} =& \frac{\alpha(\alpha^2 r - 6\alpha r - 2\alpha + 8r + 5)}{4r^2\begin{pmatrix}2\alpha^3 r^2 - 16\alpha^2 r^2 - 6\alpha^2 r + 38\alpha r^2\\ +33\alpha r - 24r^2 + 6\alpha - 36r - 12\end{pmatrix}},\\
\gamma_{1,1} =& -\frac{\alpha(2r+1)(2\alpha^2 r - 12\alpha r - 2a + 16r + 5)}{r^2(r+2)\begin{pmatrix}2\alpha^3 r^2 - 16\alpha^2 r^2 - 6\alpha^2 r + 38\alpha r^2\\ +33\alpha r - 24r^2 + 6\alpha - 36r - 12\end{pmatrix}},\\
\gamma_{2,1} =& -\frac{\begin{pmatrix}6\alpha^3 r^4 + 3\alpha^3 r^3 - 50\alpha^2 r^4 - 6\alpha^3 r^2\\ -39\alpha^2 r^3 + 128\alpha r^4 - 3\alpha^3 r + 33\alpha^2 r^2\\ +144\alpha r^3 - 96r^4 + 24\alpha^2 r - 18\alpha r^2\\ -144r^3 + 2\alpha^2 - 39\alpha r - 48r^2 - 5\alpha\end{pmatrix}}{4r^2\begin{pmatrix}2\alpha^3 r^2 - 16\alpha^2 r^2 - 6\alpha^2 r + 38\alpha r^2\\ +33\alpha r - 24r^2 + 6\alpha - 36r - 12\end{pmatrix}},\\
\gamma_{4,1} =& -\frac{\alpha(2r+1)\begin{pmatrix}\alpha^2 r^2 - 7\alpha r^2 + 12r^2\\ -3\alpha r + 12r + 3\end{pmatrix}}{4(r+2)\begin{pmatrix}2\alpha^3 r^2 - 16\alpha^2 r^2 - 6\alpha^2 r + 38\alpha r^2\\ +33\alpha r - 24r^2 + 6\alpha - 36r - 12\end{pmatrix}},\\
\beta_1 =& -\frac{(2r^2 + 3r + 1)\Gamma(5-\alpha)}{2\begin{pmatrix}2\alpha^3 r^2 - 16\alpha^2 r^2 - 6\alpha^2 r + 38\alpha r^2\\ +33\alpha r - 24r^2 + 6\alpha - 36r - 12\end{pmatrix}}.
\end{aligned} \tag{7}$$

To obtain the coefficients for the second point of the method, y_{n+2}, the unknowns of $\gamma_{4,2}$ and i in the system of equation (6) are set to be 1 and 2, respectively. Then, the value of r in the coefficients is substituted with 1, 2, and 10/19. Therefore, the VS2FBBDF(4) method is given as follows for $r = 1$, $r = 2$, and $r = 10/19$:

1) For $r = 1$:

$$\begin{aligned}
y_{n+1} =& -\frac{\alpha(\alpha^2 - 8\alpha + 13)}{4(2\alpha^3 - 22\alpha^2 + 77\alpha - 72)}y_{n-2}\\
&+ \frac{\alpha(6\alpha^2 - 42\alpha + 63)}{6\alpha^3 - 66\alpha^2 + 231\alpha - 216}y_{n-1}\\
&- \frac{30\alpha^2 - 210\alpha + 288}{4(2\alpha^3 - 22\alpha^2 + 77\alpha - 72)}y_n\\
&+ \frac{\alpha(3\alpha^2 - 30\alpha + 81)}{4(6\alpha^3 - 66\alpha^2 + 231\alpha - 216)}y_{n+2}\\
&- \frac{3\Gamma(5-\alpha)}{2\alpha^3 - 22\alpha^2 + 77\alpha - 72}h^{\alpha C}D^{\alpha}y_{n+1},\\
y_{n+2} =& \frac{\alpha(3\alpha^2 - 21\alpha - 36}{3\alpha^3 - 33\alpha^2 + 48\alpha + 432}y_{n-2}\\
&- \frac{8\alpha(\alpha^2 - 5\alpha - 8)}{\alpha^3 - 11\alpha^2 + 16\alpha + 144}y_{n-1}\\
&+ \frac{60\alpha^2 - 420\alpha + 144}{\alpha^3 - 11\alpha^2 + 16\alpha + 144}y_n\\
&+ \frac{8\alpha(3\alpha^2 - 39\alpha + 144)}{3\alpha^3 - 33\alpha^2 + 48\alpha + 432}y_{n+1}\\
&+ \frac{6(2^{\alpha})\Gamma(5-\alpha)}{\alpha^3 - 11\alpha^2 + 16\alpha + 144}h^{\alpha C}D^{\alpha}y_{n+2}.
\end{aligned} \tag{8}$$

2) For $r = 2$:

$$\begin{aligned}
y_{n+1} =& -\frac{\alpha(2\alpha^2 - 14\alpha + 21)}{16(8\alpha^3 - 76\alpha^2 + 224\alpha - 180)}y_{n-2}\\
&+ \frac{\alpha(20\alpha^2 - 130\alpha + 185)}{4(32\alpha^3 - 304\alpha^2 + 896\alpha - 720)}y_{n-1}\\
&+ \frac{90\alpha^3 - 930\alpha^2 + 3045\alpha - 2880}{16(8\alpha^3 - 76\alpha^2 + 224\alpha - 180)}y_n\\
&+ \frac{\alpha(20\alpha^2 - 170\alpha + 375)}{4(32\alpha^3 - 304\alpha^2 + 896\alpha - 720)}y_{n+2}\\
&- \frac{15\Gamma(5-\alpha)h^{\alpha C}D^{\alpha}y_{n+1}}{2(8\alpha^3 - 76\alpha^2 + 224\alpha - 180)},\\
y_{n+2} =& \frac{\alpha(8\alpha^2 - 40\alpha - 64)}{4(20\alpha^3 - 160\alpha^2 + 80\alpha + 1440)}y_{n-2}\\
&- \frac{2\alpha(2\alpha^2 - 8\alpha - 12)}{(4\alpha^3 - 32\alpha^2 + 16\alpha + 288)}y_{n-1}\\
&+ \frac{72\alpha^3 - 840\alpha^2 + 2784\alpha - 1152}{4(4\alpha^3 - 32\alpha^2 + 16\alpha + 288)}y_n\\
&+ \frac{8\alpha(16\alpha^2 - 160\alpha + 432)}{20\alpha^3 - 160\alpha^2 + 80\alpha + 1440}y_{n+1}\\
&+ \frac{12(2^{\alpha})\Gamma(5-\alpha)h^{\alpha C}D^{\alpha}y_{n+2}}{4\alpha^3 - 32\alpha^2 + 16\alpha + 288}.
\end{aligned} \tag{9}$$

3) For $r = 10/19$:

$$
\begin{aligned}
y_{n+1} =& \\
&- \frac{6859\alpha(10\alpha^2 - 98\alpha + 175)y_{n-2}}{400\,(200\alpha^3 - 2740\alpha^2 + 12236\alpha - 13572)} \\
&+ \frac{6859\alpha(780\alpha^2 - 6162\alpha + 9945)y_{n-1}}{100(9600\alpha^3 - 131520\alpha^2 + 587328\alpha - 651456)} \\
&- \frac{305370\alpha^3 - 1857102\alpha^2 - 39585\alpha + 5428800}{400(200\alpha^3 - 2740\alpha^2 + 12236\alpha - 13572)} y_n \\
&+ \frac{\alpha(3900\alpha^2 - 49530\alpha + 177957)y_{n+2}}{4(9600\alpha^3 - 131520\alpha^2 + 587328\alpha - 651456)} \\
&- \frac{1131\Gamma(5-\alpha)h^{\alpha C}D^{\alpha}y_{n+1}}{2(200\alpha^3 - 2740\alpha^2 + 12236\alpha - 13572)}, \\
y_{n+2} =& \\
&\frac{6859\alpha(480\alpha^2 - 5088\alpha - 9216)y_{n-2}}{100(3900\alpha^3 - 63960\alpha^2 + 205608\alpha + 1302912)} \\
&- \frac{13718\alpha(10\alpha^2 - 68\alpha - 116)y_{n-1}}{25(100\alpha^3 - 1640\alpha^2 + 5272\alpha + 33408)} + \\
&\frac{375840\alpha^3 - 1188768\alpha^2 - 14153856\alpha + 3340800}{100(100\alpha^3 - 1640\alpha^2 + 5272\alpha + 33408)} y_n \\
&+ \frac{8\alpha(4800\alpha^2 - 88320\alpha + 484416)y_{n+1}}{3900\alpha^3 - 63960\alpha^2 + 205608\alpha + 1302912} \\
&+ \frac{1392(2^{\alpha})\Gamma(5-\alpha)h^{\alpha C}D^{\alpha}y_{n+2}}{100\alpha^3 - 1640\alpha^2 + 5272\alpha + 33408}.
\end{aligned} \tag{10}
$$

III. Analysis of the Method

Numerous researchers have conducted analyses of the properties of the BBDF method [24]–[26] by examining the method's stability properties and convergence characteristics. Thus, the following subsection will present how to determine the order and error constant of the VS2FBBDF(4) method, as these results will be utilized in the subsequent process.

A. Order and Error Constant

The order and error constant for variable step size will be figured out by employing the subsequent definition. Basically, the formula to determine the order and error constant for the method is identical to the method used to determine the coefficient of the method [27].

Definition 1: [23] FLMM (8)-(10) are considered to have an order of p if, in (12), $C_0 = C_1 = \cdots = C_p = 0, C_{p+1} \neq 0$ where,

$$
\begin{aligned}
C_0(n,\alpha) =& \sum_{j=0}^{n} \gamma_j, \\
C_p(n,\alpha) =& \sum_{j=0}^{2} \frac{((j-2)r)^p}{p!}\gamma_j + \sum_{j=3}^{n} \frac{(j-2)^p}{p!}\gamma_j \\
&- \frac{1}{\Gamma(p+1+\alpha)} \sum_{j=0}^{n} (j-2)^{p-\alpha}\,\beta_j,
\end{aligned} \tag{11}
$$

where $p = 1, 2, 3, \cdots$. By employing Definition 1 in this part, the order and error constant of VS2FBBDF(4) method can be determined by substituting $n = 4$ in (11). Then the calculation is demonstrated below.

$$
\begin{aligned}
C_0(4,\alpha) =& \sum_{j=0}^{4} \gamma_j = \begin{bmatrix} 0 \\ 0 \end{bmatrix}, \\
C_1(4,\alpha) =& \sum_{j=0}^{2} ((j-2)r)\,\gamma_j + \sum_{j=3}^{4} (j-2)\,\gamma_j \\
&- \sum_{j=0}^{4} \frac{(j-2)^{1-\alpha}}{\Gamma(2+\alpha)}\beta_j = \begin{bmatrix} 0 \\ 0 \end{bmatrix}, \\
C_2(4,\alpha) =& \sum_{j=0}^{2} \frac{((j-2)r)^2}{2!}\gamma_j + \sum_{j=3}^{4} \frac{(j-2)^2}{2!}\gamma_j \\
&- \sum_{j=0}^{4} \frac{(j-2)^{2-\alpha}}{\Gamma(3+\alpha)}\beta_j = \begin{bmatrix} 0 \\ 0 \end{bmatrix}, \\
C_3(4,\alpha) =& \sum_{j=0}^{2} \frac{((j-2)r)^3}{3!}\gamma_j + \sum_{j=3}^{4} \frac{(j-2)^3}{3!}\gamma_j \\
&- \sum_{j=0}^{4} \frac{(j-2)^{3-\alpha}}{\Gamma(4+\alpha)}\beta_j = \begin{bmatrix} 0 \\ 0 \end{bmatrix}, \\
C_4(4,\alpha) =& \sum_{j=0}^{4} \frac{((j-2)r)^4}{4!}\gamma_j + \sum_{j=3}^{4} \frac{(j-2)^4}{4!}\gamma_j \\
&- \sum_{j=0}^{4} \frac{(j-2)^{4-\alpha}}{\Gamma(5+\alpha)}\beta_j = \begin{bmatrix} 0 \\ 0 \end{bmatrix}, \\
C_5(4,\alpha) =& \sum_{j=0}^{2} \frac{((j-2)r)^5}{5!}\gamma_j + \sum_{j=3}^{4} \frac{(j-2)^5}{5!}\gamma_j \\
&- \sum_{j=0}^{4} \frac{(j-2)^{5-\alpha}}{\Gamma(6+\alpha)}\beta_j = \begin{bmatrix} E_1 \\ E_2 \end{bmatrix} \neq \begin{bmatrix} 0 \\ 0 \end{bmatrix},
\end{aligned} \tag{12}
$$

where E_1 and E_2 denote the error constant for the first point, y_{n+1}, and the second point, y_{n+2}, respectively. By using the calculation outlined in equation (12), the results are

1) When $\alpha = 0.90$
   - For $r = 1$,
     $$E_1 = \frac{39961}{868380}, \quad \text{and} \quad E_2 = -\frac{284578}{3421655}.$$
   - For $r = 2$,
     $$E_1 = \frac{6349}{38868}, \quad \text{and} \quad E_2 = -\frac{286076}{1591005}.$$
   - For $r = 10/19$,
     $$E_1 = \frac{537341}{29305980}, \quad \text{and} \quad E_2 = -\frac{8025808}{159683315}.$$
2) When $\alpha = 0.92$
   - For $r = 1$,
     $$E_1 = \frac{4689953}{96811940}, \quad \text{and} \quad E_2 = -\frac{4272043}{49867205}.$$
   - For $r = 2$,
     $$E_1 = \frac{5941981}{34017952}, \quad \text{and} \quad E_2 = -\frac{17160944}{92553695}.$$
   - For $r = 10/19$,
     $$E_1 = \frac{6579355367}{343539931760}, \quad \text{and}$$
     $$E_2 = -\frac{9164494624}{177148401995}.$$

3) When $\alpha = 0.94$
   - For $r = 1$,
   $$E_1 = \frac{75101723}{1471583540}, \quad \text{and} \quad E_2 = -\frac{560084054}{6350135365}.$$
   - For $r = 2$,
   $$E_1 = \frac{23709949}{126659008}, \quad \text{and} \quad E_2 = -\frac{561892708}{2940192115}.$$
   - For $r = 10/19$,
   $$E_1 = \frac{911158027}{45539774560}, \quad \text{and}$$
   $$E_2 = -\frac{10366869712}{194777129435}.$$
4) When $\alpha = 0.96$
   - For $r = 1$,
   $$E_1 = \frac{1173677}{21811960}, \quad \text{and} \quad E_2 = -\frac{2239724}{24675815}.$$
   - For $r = 2$,
   $$E_1 = \frac{738602}{3672259}, \quad \text{and} \quad E_2 = -\frac{4489196}{22801255}.$$
   - For $r = 10/19$,
   $$E_1 = \frac{43608721}{2085751505}, \quad \text{and} \quad E_2 = -\frac{63331592}{1157089835}.$$
5) When $\alpha = 0.98$
   - For $r = 1$,
   $$E_1 = \frac{75081083}{1322112340}, \quad \text{and} \quad E_2 = -\frac{587320468}{2896828415}.$$
   - For $r = 2$,
   $$E_1 = \frac{2943038}{13578421}, \quad \text{and} \quad E_2 = -\frac{586675334}{6283628165}.$$
   - For $r = 10/19$,
   $$E_1 = \frac{6647305847}{304149831910}, \quad \text{and}$$
   $$E_2 = -\frac{315480029648}{5607396652115}.$$
6) When $\alpha = 1.00$
   - For $r = 1$,
   $$E_1 = \frac{3}{50} \quad \text{and} \quad E_2 = -\frac{12}{125}.$$
   - For $r = 2$,
   $$E_1 = \frac{15}{64} \quad \text{and} \quad E_2 = -\frac{24}{115}.$$
   - For $r = 10/19$,
   $$E_1 = \frac{426387}{18656480} \quad \text{and} \quad E_2 = -\frac{322944}{5586475}.$$

Referring to the results above, the error constants obtained are presented at C_5. Thus, the method is of order 4.

B. Convergence of the Method

Theorem 1: [25] FLMM (8)-(10) is convergent if and only if it satisfies the following conditions:

1) consistency, and
2) zero stability.

Definition 2: [25] FLMM (8)-(10) is considered consistent if its order is greater than or equal to p, where $p \geq 1$.

Convergence is an essential characteristic that must be considered during the development of an LMM. The purpose of this is to verify that the developed method can accurately approximate a solution to any desired level of accuracy [7]. Since we have demonstrated that the method is of order $p = 4$, which is greater than or equal to 1, we can conclude that the method is consistent, as defined in Definition 2. Next, the discussion focuses on the zero stability of the method in order to establish the second characteristic of Theorem 1.

Definition 3: FLMM (8)-(10) is considered to be zero stable when all roots of the characteristic polynomial have moduli equal to or greater than one, and each root with a modulus of one is a simple root.

The VS2FBBDF(4) method (8)–(10) is transformed into a general form of the method for all values of r, which results in

$$\begin{aligned} y_{n+1} =& A_0 y_{n-2} + A_1 y_{n-1} + A_2 y_n + A_3 y_{n+2} \\ &+ B_1 h^{\alpha\, C} D^{\alpha} y_{n+1}, \\ y_{n+2} =& A_4 y_{n-2} + A_5 y_{n-1} + A_6 y_n + A_7 y_{n+1} \\ &+ B_2 h^{\alpha\, C} D^{\alpha} y_{n+2}. \end{aligned} \tag{13}$$

By applying the test equation, ${}^{C}D^{\alpha} y(t) = \lambda y(t)$ into equation (13) where $\lambda \in \mathbb{C}$, and $Re(\lambda) < 0$, yielding the following form;

$$\begin{aligned} y_{n+1} =& A_0 y_{n-2} + A_1 y_{n-1} + A_2 y_n + A_3 y_{n+2} \\ &+ B_1 h^{\alpha} \lambda y_{n+1}, \\ y_{n+2} =& A_4 y_{n-2} + A_5 y_{n-1} + A_6 y_n + A_7 y_{n+1} \\ &+ B_2 h^{\alpha} \lambda y_{n+2}. \end{aligned} \tag{14}$$

By substituting the actual values $h^{\alpha}\lambda = H$ into equation (14), we obtain the equation in a matrix form as:

$$\begin{aligned} &\begin{bmatrix} 1 - B_1 H & -A_3 \\ -A_7 & 1 - B_2 H \end{bmatrix} \begin{bmatrix} y_{n+1} \\ y_{n+2} \end{bmatrix} \\ &= \begin{bmatrix} A_1 & A_2 \\ A_5 & A_6 \end{bmatrix} \begin{bmatrix} y_{n-1} \\ y_n \end{bmatrix} + \begin{bmatrix} 0 & A_0 \\ 0 & A_4 \end{bmatrix} \begin{bmatrix} y_{n-3} \\ y_{n-2} \end{bmatrix}, \end{aligned} \tag{15}$$

which is similar to $PY_m = QY_{m-1} + RY_{m-2}$ where

$$\begin{aligned} &P = \begin{bmatrix} 1 - B_1 H & -A_3 \\ -A_7 & 1 - B_2 H \end{bmatrix}, \quad Q = \begin{bmatrix} A_1 & A_2 \\ A_5 & A_6 \end{bmatrix}, \\ &R = \begin{bmatrix} 0 & A_0 \\ 0 & A_4 \end{bmatrix}, \quad Y_m = \begin{bmatrix} y_{n+1} \\ y_{n+2} \end{bmatrix}, \quad Y_{m-1} = \begin{bmatrix} y_{n-1} \\ y_n \end{bmatrix}, \\ &Y_{m-2} = \begin{bmatrix} y_{n-3} \\ y_{n-2} \end{bmatrix}. \end{aligned} \tag{16}$$

The stability polynomial of the method is then determined

by applying the formula

$$\pi(x;H) = \det\left|Px^2 - Qx - R\right| = \det\left|\begin{bmatrix} 1-B_1H & -A_3 \\ -A_7 & 1-B_2H \end{bmatrix} x^2 - \begin{bmatrix} A_1 & A_2 \\ A_5 & A_6 \end{bmatrix} x - \begin{bmatrix} 0 & A_0 \\ 0 & A_4 \end{bmatrix}\right|. \tag{17}$$

By substituting $H = 0$ into equation (17), we determine the zero stability, resulting in:

1) When $\alpha = 0.90$:
   - $r = 1$: Roots, $x_s = 0, 1, -0.2669$, and 0.01574.
   - $r = 2$: Roots, $x_s = 0, 0.002303, 1$, and -0.05935.
   - $r = 10/19$: Roots, $x_s = 0, 0.06876, 1$, and -0.9946.
2) When $\alpha = 0.92$:
   - $r = 1$: Roots, $x_s = 0, 0.01661, 1$, and -0.2633.
   - $r = 2$: Roots, $x_s = 0, 0.002459, 1$, and -0.05833.
   - $r = 10/19$: Roots, $x_s = 0, 0.07187, 1$, and -0.9854.
3) When $\alpha = 0.94$:
   - $r = 1$: Roots, $x_s = 0, 0.01755, 1$, and -0.2593.
   - $r = 2$: Roots, $x_s = 0, 0.002630, 1$, and -0.05716.
   - $r = 10/19$: Roots, $x_s = 0, 0.07512, 1$, and -0.9748.
4) When $\alpha = 0.96$:
   - $r = 1$: Roots, $x_s = 0, 0.01856, 1$, and -0.2547.
   - $r = 2$: Roots, $x_s = 0, 0.002819, 1$, and -0.05584.
   - $r = 10/19$: Roots, $x_s = 0, 0.07852, 1$, and -0.9628.
5) When $\alpha = 0.98$:
   - $r = 1$: Roots, $x_s = 0, 0.01963, 1$, and -0.2497.
   - $r = 2$: Roots, $x_s = 0, 0.003027, 1$, and -0.05435.
   - $r = 10/19$: Roots, $x_s = 0, 0.08208, 1$, and -0.9494.
6) When $\alpha = 1.00$:
   - $r = 1$: Roots, $x_s = 0, 1, -0.2442$, and 0.0208.
   - $r = 2$: Roots, $x_s = 0, 1, -0.05272$, and 0.00326.
   - $r = 10/19$: Roots, $x_s = 0, 1, -0.9346$, and 0.0858.

The VS2FBBDF(4) method (8)-(10) has been demonstrated to be zero-stable, with the condition that the absolute value of the roots, $|x_s| \leq 1$, and it satisfies the criteria outlined in Definition 3. As a result, the VS2FBBDF(4) method (8)-(10) is convergent. Subsequently, the method's stability regions will be examined in the following subsection.

C. Stability Properties

This subsection primarily investigates the stability properties of method (8)-(10) and the values of fractional-order, α, in the method is restricted to the (0,1]. To make a comparison with the existing method, the stability of the proposed method will be studied for α in between 0.90 and 1.00. Some important stability requirements for a numerical method are examined, including A-stable, and absolutely-stable.

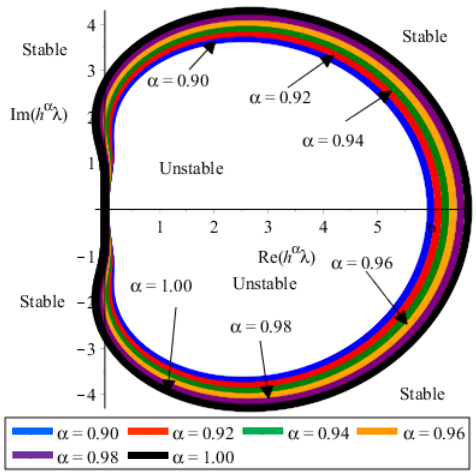

Fig. 2. Stability region of the method for $r = 1$ with $\alpha \in [0.90, 1.00]$.

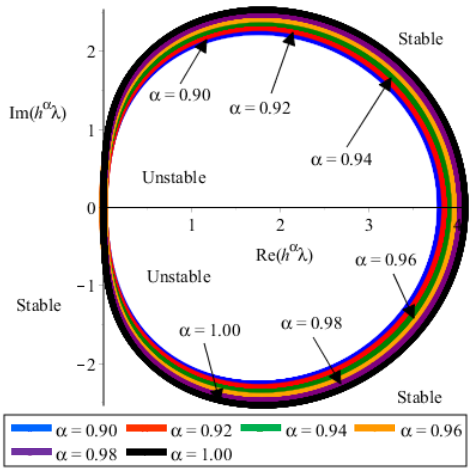

Fig. 3. Stability region of the method for $r = 2$ with $\alpha \in [0.90, 1.00]$.

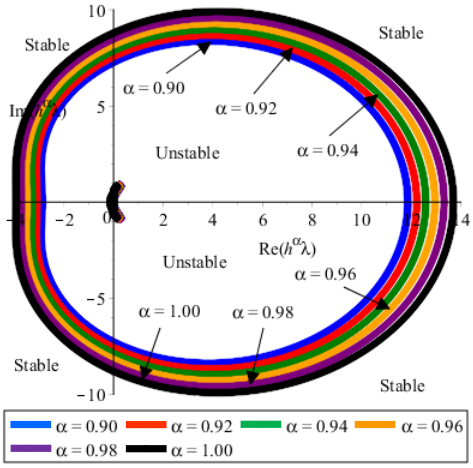

Fig. 4. Stability region of the method for $r = 10/19$ with $\alpha \in [0.90, 1.00]$.

Definition 4: FLMM (8)-(10) is claimed to be absolutely-stable in a region R for a given $h^\alpha\lambda = H$ if for that H, all the roots, x_s of the stability polynomial (17) satisfy $|x_s| < 1$ where $s = 1, 2, \cdots, k$.

Definition 5: [25] FLMM (8)-(10) is claimed to be A-stable if the absolute stability regions cover the whole left half plane.

Following that, a series of numerical experiments were performed to demonstrate the region of the graphs in Figures 2-4 that are absolutely stable. According to the analysis, the stable regions are located outside the circles. Thus, it can be inferred that the VS2FBBDF(4) method (8)-(9) is A-stable for $\alpha \in [0.90, 1.00]$ as the region of absolute stability completely encompasses the entire left half-plane. Meanwhile, the method (10) is almost A-stable for $\alpha \in [0.90, 1.00]$ as the region of absolute stability almost covered the region, R, on the entire left half-plane.

IV. Results and Discussion

This section presents numerical simulations to validate the analytical method introduced in the previous section. The values and parameters in Table I are considered to obtain the numerical results. In order to assess the effectiveness of the VS2FBBDF(4) method (8)-(10), the numerical outcomes are compared with those obtained by the established methods, as outlined in Tables II-III.

The 2FBBDF(4) [23] and VS2FBBDF(4) methods were calculated using C++ programming, while the numerical outcomes for fourth-kind Chebyshev wavelets (FKCW) and Müntz-Legendre polynomials (MLP) methods were acquired from [8] and [28], respectively. Table II displays the numerical solution of model (2) when integer order is taken into consideration. Since the model (2) does not have the exact solution, we consider the Maple solution as the true value in order to compute the absolute error, ABERR. Thus, the following equation represents the formula for ABERR.

$$\text{ABERR}_i = |y_i(t) - y_i(t_n)|, \quad i = 1, 2, \cdots, n \in \mathbb{Z}^+, \quad (18)$$

where i is the number of iterations, $y_i(t)$ is the Maple solution, and $y_i(t_n)$ is the approximate solution. Next, the outcomes presented in Table II are depicted in Figures 5-7 to demonstrate the pattern of the proposed method, the 2FBBDF(4) method, the FKCW method, and the solution from Maple software, which is used as a tool to verify the solution of the model (2). As shown in the figures, the 2FBBDF(4) and VS2FBBDF(4) methods approximate the solutions closer to the computed line compared to the FKCW method. However, the 2FBBDF(4) method appears unstable because the plotted solution is not aligned with the Maple solution.

Figures 8-10 present the efficiency curves that compare the computational performance of the VS2FBBDF(4) method against the 2FBBDF(4) and FKCW methods when solving the model with an integer order of $\alpha = 1.00$. This comparison indicates that the 2FBBDF(4) and VS2FBBDF(4) methods provides more accurate results at $\alpha = 1.00$ compared to the FKCW method for $t \in [0, 1]$. The solution is constrained to $t \in [0, 1]$ because the code to generate the solution beyond this interval is not accessible. Hence, the values reported in the paper were utilized. Concurrently, the solution for 2FBBDF(4) can be generated for the time interval $t \in [0, 4]$. It can be observed that the variable step method demonstrates better accuracy compared to the fixed step method.

Next, the fractional model (2) is computed using the VS2FBBDF(4) method with a fractional order of $\alpha = 0.90$. The resulting values are presented in Table III along with

TABLE II
The solutions of the mathematical model (2) for $\alpha = 1.00$.

t	Method	$T(t)$	$I(t)$	$V(t)$
0	FKCW	1.00000e-01	0.00000e+00	1.00000e-01
	2FBBDF(4)	1.00000e-01	0.00000e+00	1.00000e-01
	VS2FBBDF(4)	1.00000e-01	0.00000e+00	1.00000e-01
	MAPLE	1.00000e-01	0.00000e+00	1.00000e-01
0.2	FKCW	2.10286e-01	6.09955e-06	6.19989e-02
	2FBBDF(4)	2.08288e-01	6.00695e-06	6.18038e-02
	VS2FBBDF(4)	2.08808e-01	6.03269e-06	6.18798e-02
	MAPLE	2.07668e-01	5.99150e-06	6.17004e-02
0.4	FKCW	4.09688e-01	1.32894e-05	3.83340e-02
	2FBBDF(4)	4.05139e-01	1.31118e-05	3.82478e-02
	VS2FBBDF(4)	4.06242e-01	1.31582e-05	3.82946e-02
	MAPLE	4.02100e-01	1.30162e-05	3.80731e-02
0.6	FKCW	7.72069e-01	2.14336e-05	2.37077e-02
	2FBBDF(4)	7.62126e-01	2.11651e-05	2.36754e-02
	VS2FBBDF(4)	7.64221e-01	2.12202e-05	2.37038e-02
	MAPLE	7.53158e-01	2.09056e-05	2.34989e-02
0.8	FKCW	1.43043e+00	3.04824e-05	1.46692e-02
	2FBBDF(4)	1.40932e+00	3.01294e-05	1.46623e-02
	VS2FBBDF(4)	1.41402e+00	3.01699e-05	1.46762e-02
	MAPLE	1.38683e+00	2.95926e-05	1.45107e-02
1.0	FKCW	2.62537e+00	4.04365e-05	9.10335e-03
	2FBBDF(4)	2.58201e+00	4.00484e-05	9.08966e-03
	VS2FBBDF(4)	2.59001e+00	4.00115e-05	9.09656e-03
	MAPLE	2.53003e+00	3.90783e-05	8.96951e-03

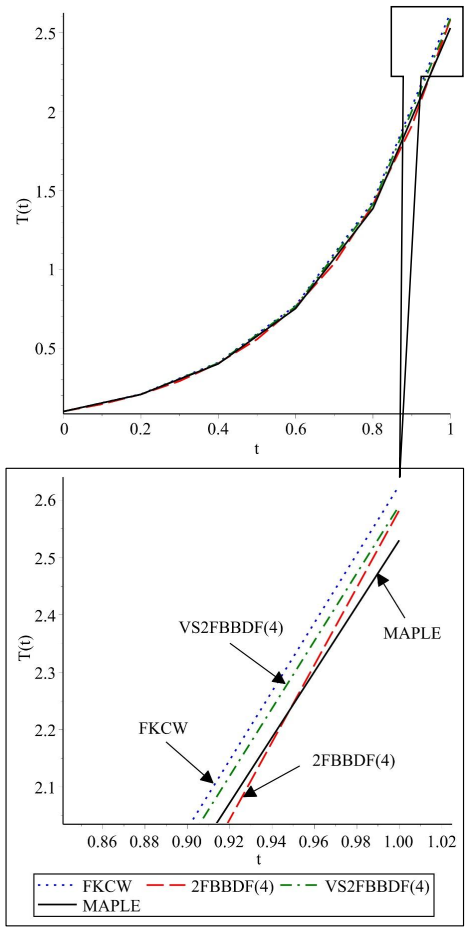

Fig. 5. Graph comparing methods for $T(t)$ when $\alpha = 1.00$.

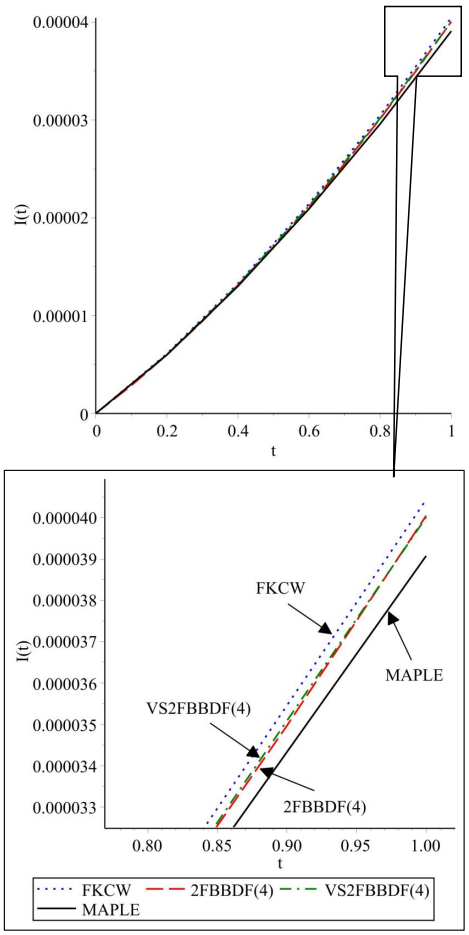

Fig. 6. Graph comparing methods for $I(t)$ when $\alpha = 1.00$.

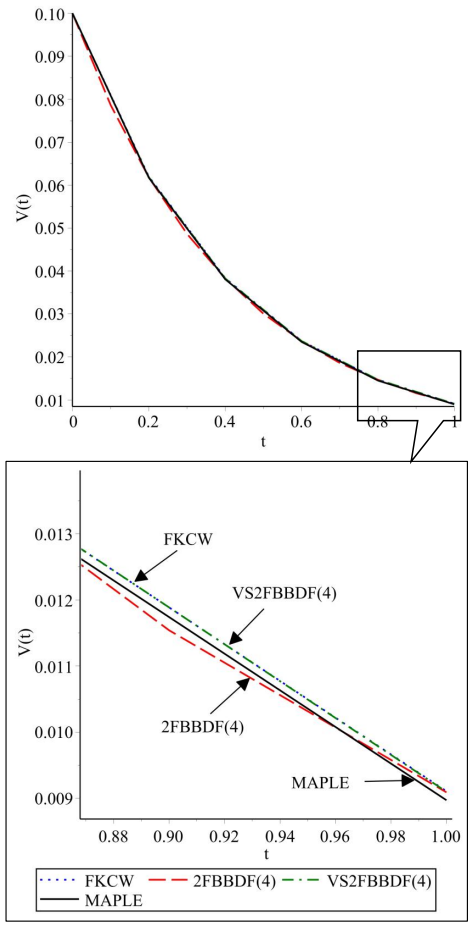

Fig. 7. Graph comparing methods for $V(t)$ when $\alpha = 1.00$.

the numerical results obtained from the MLP and FKCW methods, and the results are illustrated in Figures 11-13.

As presented in Figures 11-13, comparing all the methods reveals a consistent pattern that aligns with the Maple solutions. It should be noted that the solution generated by Maple is in Figure 11, the VS2FBBDF(4) method provides a larger approximation of the solution $T(t)$ compared to the methods of comparison. Additionally, the VS2FBBDF(4) method provides smaller approximations of the solutions $I(t)$ and $V(t)$ compared to the methods of comparison. The graphs' behavior indicates that the method converges towards the Maple solution, as depicted in Figures 12-13.

Figures 11-13 illustrate that the comparison of all methods demonstrates a consistent trend, with the numerical solutions closely aligning with the Maple solution, especially for the 2FBBDF(4) method. Of all the evaluated methods, 2FBBDF(4) exhibits superior accuracy across all subplots, closely aligning its trajectories with the Maple curves for $T(t)$, $I(t)$, and $V(t)$. Nevertheless, additional analysis is required to thoroughly assess the efficacy of each method in solving the fractional model (2) for $\alpha = 0.9$.

Concerning the comparison methods, the VS2FBBDF(4) method yields a significantly larger approximation of $T(t)$ than the others, as illustrated in Figure 11. This behavior may be ascribed to a minor overestimation of the actual solution in this issue.

Figures 12-13 demonstrate that the MLP and FKCW methods exhibit inconsistencies after $t = 0.6$, with their

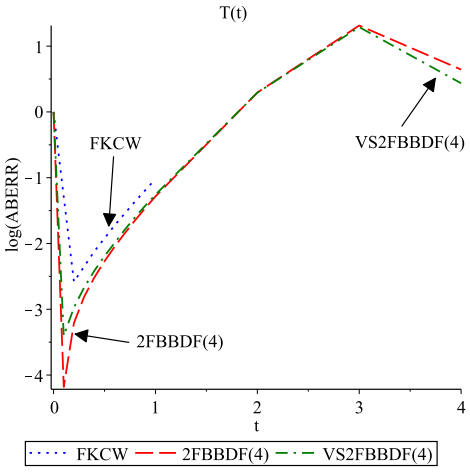

Fig. 8. Efficiency curves for $T(t)$ when $\alpha = 1.00$.

curves beginning to deviate significantly from the Maple solution. Conversely, the 2FBBDF(4) and VS2FBBDF(4) methods maintain alignment with the Maple curve for the compartments $I(t)$ and $V(t)$.

This analysis indicates that the VS2FBBDF(4) method is more advantageous for solving the fractional model, due to the consistency and stability of its solutions compared to the MLP and FKCW methods. Additionally, the effectiveness in capturing the memory effects, the computational efficiency and performance of the 2FBBDF(4) and VS2FBBDF(4)

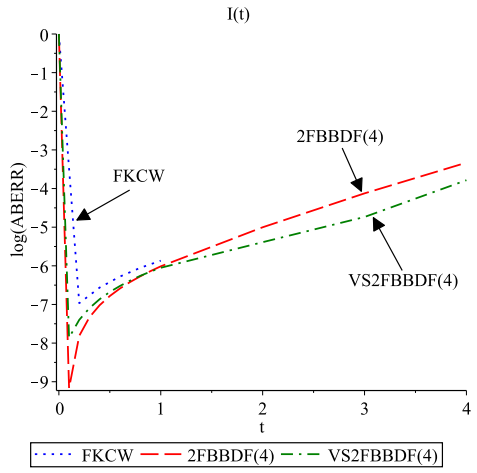

Fig. 9. Efficiency curves for $I(t)$ when $\alpha = 1.00$.

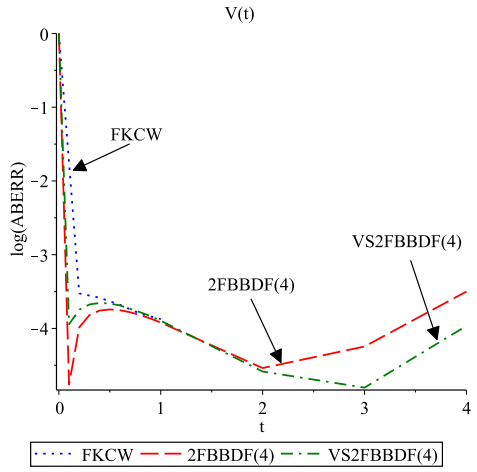

Fig. 10. Efficiency curves for $V(t)$ when $\alpha = 1.00$.

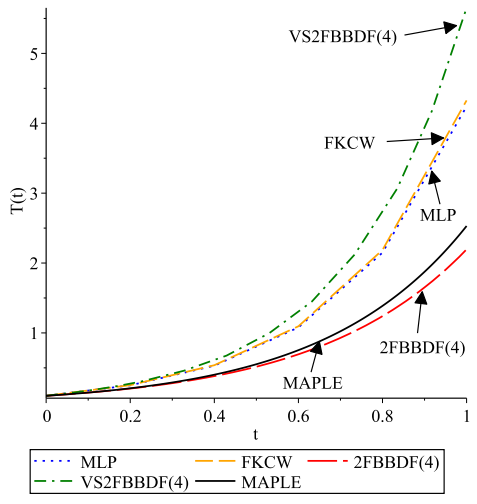

Fig. 11. Graph comparing methods for $T(t)$ when $\alpha = 0.90$.

methods with $\alpha = 0.90$ will be examined further in the subsequent figures.

Figures 14-16 illustrates the memory effects for $\alpha \in [0.90, 1.00]$ values. Figure 14 demonstrates an increase in the concentration of susceptible T cells over time, as indicated by the observed data. Upon infection of CD4$^+$T cells with

TABLE III
THE SOLUTIONS OF THE MATHEMATICAL MODEL (2) FOR $\alpha = 0.90$.

t	Method	$T(t)$	$I(t)$	$V(t)$
0	MLP	1.00000e-01	0.00000e+00	1.00000e-01
	FKCW	1.00000e-01	0.00000e+00	1.00000e-01
	2FBBDF(4)	1.00000e-01	0.00000e+00	1.00000e-01
	VS2FBBDF(4)	1.00000e-01	0.00000e+00	1.00000e-01
0.2	MLP	2.50116e-01	7.76924e-06	5.67019e-02
	FKCW	2.52768e-01	7.89591e-06	5.68077e-02
	2FBBDF(4)	2.04161e-01	5.81088e-06	6.22635e-02
	VS2FBBDF(4)	2.74649e-01	8.76520e-06	5.16876e-02
0.4	MLP	5.30988e-01	1.67537e-05	3.58789e-02
	FKCW	5.37760e-01	1.69991e-05	3.58936e-02
	2FBBDF(4)	3.83358e-01	1.24271e-05	3.97642e-02
	VS2FBBDF(4)	6.09259e-01	1.82731e-05	2.96256e-02
0.6	MLP	1.07850e+00	2.81650e-05	2.40146e-02
	FKCW	1.09486e+00	2.85826e-05	2.40055e-02
	2FBBDF(4)	6.96496e-01	1.99079e-05	2.53896e-02
	VS2FBBDF(4)	1.29687e+00	2.95340e-05	1.71539e-02
0.8	MLP	2.14892e+00	4.34646e-05	1.68397e-02
	FKCW	2.18700e+00	4.41504e-05	1.68260e-02
	2FBBDF(4)	1.24674e+00	2.82923e-05	1.62198e-02
	VS2FBBDF(4)	2.72148e+00	4.28239e-05	9.94345e-03
1.0	MLP	4.24091e+00	6.50302e-05	1.23158e-02
	FKCW	4.32723e+00	6.67043e-05	1.24822e-02
	2FBBDF(4)	2.20707e+00	3.76022e-05	1.02969e-02
	VS2FBBDF(4)	5.66549e+00	5.84521e-05	5.78131e-03

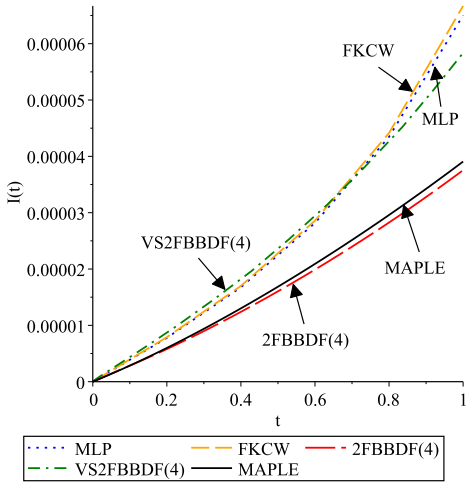

Fig. 12. Graph comparing methods for $I(t)$ when $\alpha = 0.90$.

HIV, there was a rapid decrease in the presence of HIV RNA particles in the blood, as shown in Figure 16. As depicted in Figure 15, this led to a rapidly increasing number of infected T cells.

The results demonstrated the behavior of the solution for 1 day, as previously demonstrated in Figures 5-16. In order to clarify the dynamical behavior, the fractional model (2) is solved by increasing a number of time with $t = 24$ days. Then, the results are compared to the code available in MATLAB, which is referred to as fde12.m (FDE12). This code is taken into consideration because it is accessible on the MathWorks website.

The dynamic behavior of a model that represents HIV infection of CD4$^+$T cells is illustrated in Figures 17-19.

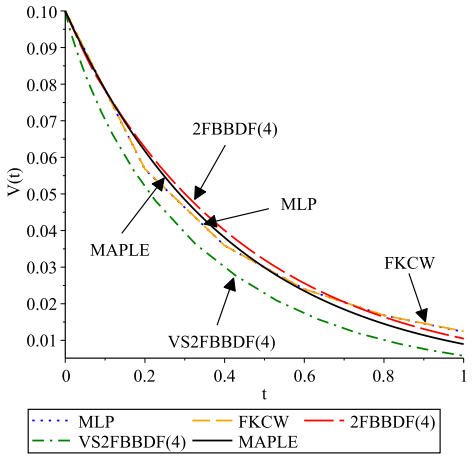

Fig. 13. Graph comparing methods for $V(t)$ when $\alpha = 0.90$.

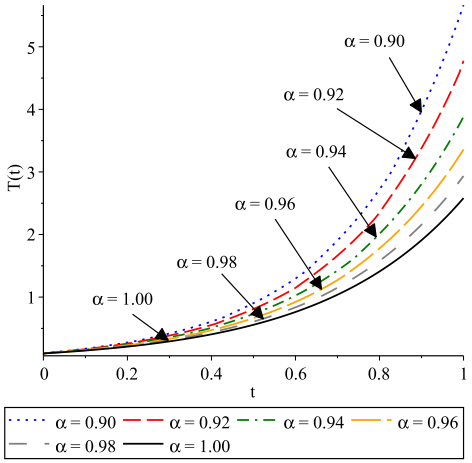

Fig. 14. The numerical behavior for $T(t)$ when $\alpha \in [0.90, 1.00]$.

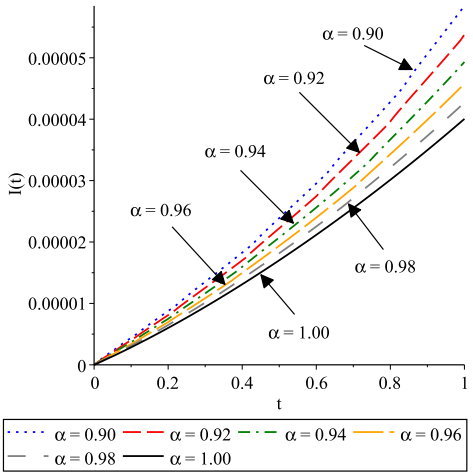

Fig. 15. The numerical behavior for $I(t)$ when $\alpha \in [0.90, 1.00]$.

The comparison involves numerical solutions obtained using the FDE12, 2FBBDF(4), and VS2FBBDF(4) methods, with the Maple solution serving as the benchmark. The fractional model (2) is solved with a fractional order of $\alpha = 0.9$. Accordingly, Figure 17 illustrates the concentration rate of healthy CD4$^+$T cells, $(T(t))$; Figure 18 shows the concentration rate of infected CD4$^+$T cells, $(I(t))$; and Figure 19

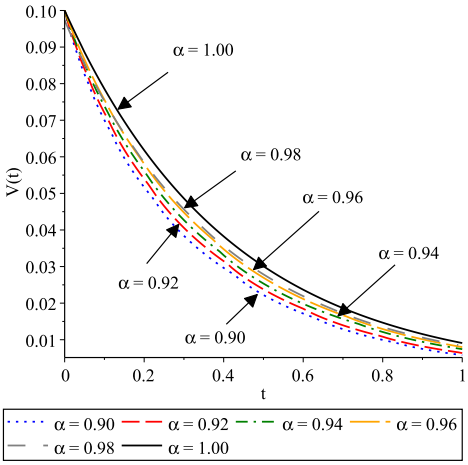

Fig. 16. The numerical behavior for $V(t)$ when $\alpha \in [0.90, 1.00]$.

presents the concentration of a virus population of CD4$^+$T cells by HIV in the blood, $(V(t))$.

As seen in Figure 17, the FDE12, 2FBBDF(4), and VS2FBBDF(4) methods initially align closely with the Maple solution. However, there is a slight divergence as time progresses, particularly around day 10 to day 18 for the FDE12 and VS2FBBDF(4) methods. It is different for the 2FBBDF(4) method, the method slightly overestimates the solution starting from day 10. Nevertheless, the VS2FBBDF(4) method generally maintains a trajectory that converges towards the Maple solution throughout the simulation.

In Figure 18, which depicts the dynamics of infected cells, $I(t)$, the VS2FBBDF(4) method exhibits a more significant phase shift compared to the FDE12 and 2FBBDF(4) methods, yet its trend continues to align closely with the Maple solution. Similarly in Figure 19, which illustrates the virus population, $V(t)$, the VS2FBBDF(4) method once again demonstrates superior agreement with the benchmark. In contrast, the FDE12 method diverges more significantly as time increases, and the 2FBBDF(4) method continues to slightly overestimate the values.

These findings indicate that the proposed method (VS2FBBDF(4)) can be considered a solution for the fractional model (2), as it effectively captures the memory effects of the model more effectively than the 2FBBDF(4) and FDE12 methods within the interval $t \in [0, 24]$ days. This emphasizes the significance of selecting suitable numerical methods for fractional-order models to guarantee the reliable simulation of complex biological systems, such as the dynamics of HIV infection. Furthermore, the pattern of memory effects must adhere to the hypothesis of stability graphs. As illustrated in Figures 2-4, the numerical solution of the model with $\alpha = 0.9$ should converge towards the Maple solution and not exceed the benchmark curves. Consequently, the analysis indicates that the VS2FBBDF(4) method is more appropriate for solving the fractional mathematical model (2) than the 2FBBDF(4) method.

V. Conclusion

As a conclusion, this study presents the derivation of a fourth-order 2-point fractional BBDF method with a variable

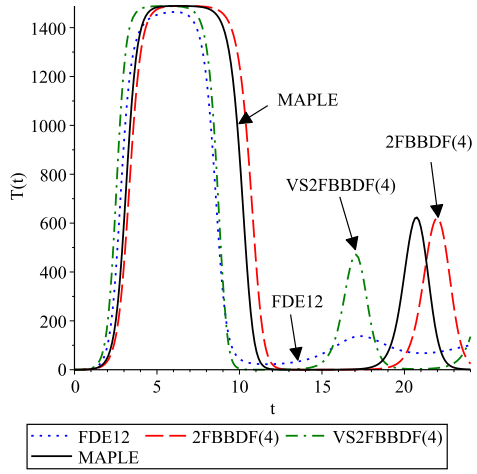

Fig. 17. The dynamical behavior for $T(t)$ when $\alpha = 0.90$.

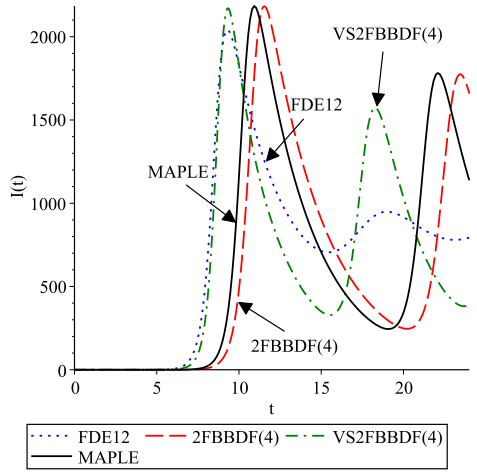

Fig. 18. The dynamical behavior for $I(t)$ when $\alpha = 0.90$.

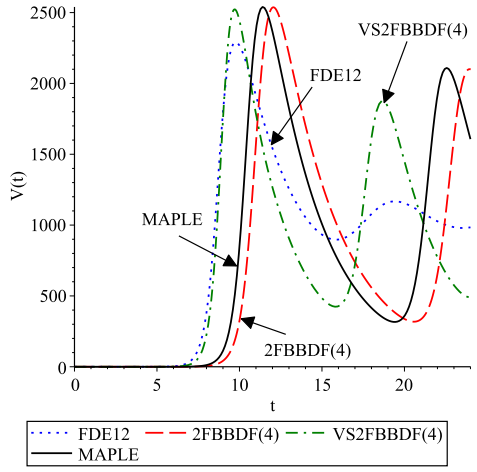

Fig. 19. The dynamical behavior for $V(t)$ when $\alpha = 0.90$.

step (VS2FBBDF(4)) to solve the fractional HIV model (2). An extensive analysis is conducted on the stability properties of the method, and the conditions that are both necessary and sufficient for its convergence are discussed. When considering various values of r, it is observed that the formula is A-stable for r equal to 1 and 2 and almost A-stable when r is equal to 10/19. According to the classical BBDF method theory, it is essential for achieving optimal performance for a numerical scheme, especially when dealing with stiff system problems, that the method be A-stable. In addition, we have examined the impact of fractional derivatives on the concentration of CD4$^+$T cells in individuals infected with HIV over time. Comparisons with alternative methods, such as the FKCW, MLP, FDE12, and 2FBBDF(4) methods, revealed that the VS2FBBDF(4) method offers enhanced precision and stability, especially in fractional models. As a result, we assert that this study is significant because it can serve as an alternative solver for acquiring numerical solutions for various types of dynamical system problems. Furthermore, the proposed method can be expanded to deal with FDEs with time delays in future research.

REFERENCES

[1] L. Wang and M. Y. Li, "Mathematical analysis of the global dynamics of a model for HIV infection of CD4$^+$T cells," *Math. Biosci.*, vol. 200, no. 1, pp. 44-57, 2006.

[2] UNAIDS, Global HIV and AIDS Statistics - Fact Sheet 2024. Available from: http://www.unaids.org/en/resources/fact-sheet [Accessed on 20th January 2025].

[3] L. Cai, X. Li, M. Ghosh and B. Guo, "Stability analysis of an HIV/AIDS epidemic model with treatment," *J. Comput. Appl. Math.*, vol. 229, no. 1, pp. 313-323, 2009.

[4] R. V. Culshaw and S. Ruan, "A delay-differential equation model of HIV infection of CD4$^+$T-cells," *Mathematical Biosciences*, vol. 165, no. 1, pp. 27-39, 2000.

[5] U. Habibah, Trisilowati, Y. L. Pradana and W. Villadystian, "Mathematical model of HIV/AIDS with two different stages of infection subpopulation and its stability analysis," *Engineering Letters*, vol. 29, no.1, pp. 1-9, 2021.

[6] S. T. Mohyud-Din, A. Nazir, B. Almohsin, N. Ahmed, U. Khan, A. Waheed and T. Hussain, "On mathematical model of HIV CD4$^+$T-cells," *Alexandria Engineering Journal*, vol. 60, no. 1, pp. 995-1000, 2021.

[7] S. J. Aksah and Z. B. Ibrahim, "Singly diagonally implicit block backward differentiation formulas for HIV infection of CD4$^+$T cells," *Symmetry*, vol. 11, no. 5, pp. 625, 2019.

[8] H. D. Azodi and M. R. Yaghouti, "A new method based on fourth kind chebyshev wavelets to a fractional-order model of HIV infection of CD4$^+$T cells," *Computational Methods for Differential Equations*, vol. 6, no. 3, pp. 353-371, 2018.

[9] A. Hyder, M. A. Barakat, D. Rizk, R. Shah and K. Nonlaopon, "Study of HIV model via recent improved fractional differential and integral operators," *AIMS Mathematics*, vol. 8, no. 1, pp. 1656-1671, 2023.

[10] A. Gökdogan, A. Yildirim and M. Merdan, "Solving a fractional-order model of HIV infection of CD4$^+$T cells," *Math. Comput. Model.*, vol. 54, no. 9-10, pp. 2132-2138, 2011.

[11] D. Baleanu and B. Shiri, "Nonlinear higher order fractional terminal value problems," *AIMS Mathematics*, vol. 7, no. 5, pp. 7489-7506, 2022.

[12] H. Najafi, S. Etemad, N. Patanarapeelert , J. K. K. Asamoah, S. Rezapour, T. Sitthiwirattham, "A study on dynamics of CD4$^+$T -cells under the effect of HIV-1 infection based on a mathematical fractal-fractional model via the adams-bashforth scheme and newton polynomials," *Mathematics*, vol. 10, no. 9, pp. 1366, 2022.

[13] H. Soomro, N. Zainuddin, H. Daud, J. Sunday, N. Jamaludin, A. Abdullah, A. Mulono, E. A. Kadir, "3-Point block backward differentiation formula with an off-step point for the solutions of stiff chemical reaction problems," *Journal of Mathematical Chemistry*, vol. 61, pp. 75-97, 2023.

[14] H. M. Ijam, Z. B. Ibrahim and I. S. M. Zawawi, "Stiffly stable diagonally implicit block backward differentiation formula with adaptive step size strategy for stiff ordinary differential equations," *Matematika*, vol. 40, no. 1, pp. 27-47, 2024.

[15] S. A. M. Yatim, A. I. Asnor and N. M. Noor, "The effect of step size ratio on 2-point block backward differentiation formula for solving stiff ODEs," *AIP Conf. Proc.*, vol. 3189, pp. 030006, 2024.

[16] M. S. Heris and M. Javidi, "On fractional backward differential formulas methods for fractional differential equations with delay," *International Journal of Applied and Computational Mathematics*, vol. 4, no. 72, 15 pages, 2018.

[17] L. Sadek, "Fractional bdf methods for solving fractional differential matrix equations," *International Journal of Applied and Computational Mathematics*, vol. 8, no. 238, 28 pages, 2022.

[18] L. Galeone and R. Garrappa, "On multistep methods for differential equations of fractional order," *Mediterranean Journal of Mathematics*, vol. 3, pp. 565-580, 2006.
[19] R. Ramesh and G. A. Joseph, "The optimal control methods for the Covid-19 pandemic model's precise and practical SIQR mathematical model," *IAENG International Journal of Applied Mathematics*, vol. 54, no. 8, pp. 1657-1672, 2024.
[20] R. Singh, A. Akgül, J. Mishra and V. K. Gupta, "Mathematical evaluation and dynamic transmission of a cervical cancer model using a fractional operator," *Contemporary Mathematics*, vol. 5, no. 3, pp. 2646-2667, 2024.
[21] B. Shiri and D. Baleanu, "Numerical solution of some fractional dynamical systems in medicine involving non-singular kernel with vector order," *Results in Nonlinear Analysis*, vol. 2, no. 4, pp. 160-168, 2019.
[22] S. A. M. Yatim, Z. B. Ibrahim, K. I. Othman and M. B. Suleiman, "Numerical solution of extended block backward differentiation formulae for solving stiff ODEs," *Proceedings of the World Congress on Engineering 2012*, vol. 1, pp. 109-113, 2012.
[23] N. M. Noor, S. A. M. Yatim and Z. B. Ibrahim, "Fractional block method for the solution of fractional order differential equations," *Malaysian Journal of Mathematical Sciences*, vol. 18, no. 1, pp. 185-208, 2024.
[24] M. Abdullahi, A. Bello and G. I. Danbaba, "Maple simulation codes for stability analysis of variable step super class of block backward differentiation formula for integrating a system of first order stiff ivps," *FUDMA Journal of Sciences*, vol. 7, no. 4, pp. 113-121, 2023.
[25] A. Buhari, Y. Hamza and A. Abdulrahman,"Analysis of convergence and stability properties of diagonally implicit 3-point block backward differentiation formula for first order stiff initial value problems," *UMYU Scientifica*, vol. 3, no. 2, pp. 186-201, 2024.
[26] H. Musa and H. Iliyasu, "Two-point diagonally implicit extended super class of block backward differentiation formula for stiff initial value problems," *Journal of Applied Sciences, Information and Computing*, vol. 3, no. 2, pp. 1-5, 2022.
[27] M. B Suleiman, H. Musa, F. Ismail, and N. Senu, "A new variable step size block backward differentiation formula for solving stiff initial value problems," *International Journal of Computer Mathematics*, vol. 90, no. 11, pp. 2391-2408, 2013.
[28] M. R. Gandomani and M. T. Kajani, "Numerical solution of a fractional order model of HIV infection of CD4$^+$T cells using Müntz-Legendre polynomials," *Int. J. Bioautomation*, vol. 20, no. 2, pp. 193-204, 2016.